

## **IN VITRO EFFECTS OF IRON NANOPARTICLES ON SCHISTOSOMA MANSONI ADULT WORMS AND ITS INTERMEDIATE HOST SNAIL, BIOMPHALARIA ALEXANDRINA**

By

**LOTFIA M. M. KHALIL<sup>1</sup>, AHMAD M. AZZAM<sup>2</sup>, HATEM A. M. MOHAMED<sup>3</sup>,  
AHMED H. NIGM<sup>3</sup>, HODA A. TAHA<sup>3</sup> AND MOHAMMAD I. SOLIMAN<sup>3\*</sup>**

Faculty of Education, El Zawia University, Lybia<sup>1</sup>, Theodor Bilharz Institute, Imbaba P. O. Box 30, Giza<sup>2</sup>, and Department of Zoology, Faculty of Science, Ain Shams University, Cairo 11566<sup>3</sup>, Egypt (\*Correspondence:solimanmi@yahoo.com)

### **Abstract**

Due to increasing problems of the resistance associated with praziquantel, the drug of choice for treatment of schistosomiasis, alternative therapies were tried. The present work evaluated the effect of iron nanoparticles (iron NPs) on *S. mansoni* and *B. alexandrina in vitro*. The mortality rate of adults was observed after exposure during a period of 48 hrs. Worms exposed to 30 & 60mg/L of iron nanoparticles showed 20% & 77% mortality after 3 hrs, respectively. Snails exposure to different concentration of iron NPs (1- 40mg/L) died (100%) at, 40mg/L after 24 hours of exposure. The commonest surface ultrastructural changes were exposing of blebs everywhere, cracks, erosion, and incomplete fusion of some tubercles that lost most of their spines. Perforation was noticed on some areas of the tegument. The ventral sucker sinks incompletely inside the tegumental surface, sloughing was observed and perforation was noticed on the body surface. Also, collapsed tegumental architecture, huge oedematous structures were lounged from collapsed tegument.

**Keywords:** *Schistosoma mansoni*, Nanoparticles, *Biomphalaria alexandrina*.

### **Introduction**

Amongst human parasitosis, schistosomiasis ranked second behind malaria in terms of socio-economic and public health importance in the tropical and subtropical areas (WHO, 2002). Schistosomiasis treatment mainly depended on praziquantel (PZQ), which was the drug of choice. However, the resistant strains of schistosomes appeared to be due to extensive use of PZQ (Cioli *et al*, 1993; Fallon and Doenhoff, 1994; Ismail *et al*, 1999; Zhang and Coultas, 2011; Ke *et al*, 2017). Therefore, investigation of new agents for treatment of schistosome's infection with the ability of high toxicity to parasites and less resistance is the issue of considerable interest. According to the National Science Foundation of USA, nanotechnology deals with controlling or restructuring of the material dimension more or less between 1 & 100nm. For various reasons related to the small size, as better solubility, absorption and uptake, nanoparticle-based medicines can get across cell membranes and reach specific targets more easily than bulk

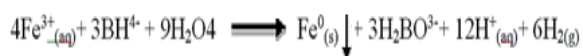
form agents (Roduner, 2006) reach. Nano-scale particles formed by metals are known as magnetic nanoparticles (MNPs) (Gupta and Gupta 2005). In the recent years, metal oxide nanoparticles have been proposed as antibacterial (Wang *et al*, 2012), antiviral (You *et al*, 2011), antifungal (Kim *et al*, 2012), antiprotozoal (Baiocco *et al*, 2010; Delavari *et al*, 2014) and anthelmintic agents (Khan *et al*, 2015; 2017) and several studies have been performed in these fields.

The present study aimed to evaluate *in-vitro* schistosomacidal activity of iron nanoparticles using SEM. In addition, the effect of iron nanoparticles on the mortality rate of *B. alexandrina* the intermediate host of *S. mansoni* was investigated.

### **Materials and Methods**

Synthesis of nano-zero valent iron particles: Nano scale zero valent iron (nZVI) particles were prepared by reduction method using two main chemicals; FeCl<sub>3</sub> & NaBH<sub>4</sub> following the method proposed by Sun *et al*. (2006). The NaBH<sub>4</sub> functions as a reducing agent for the ferric chloride FeCl<sub>3</sub> in form of

solution to produce nZVI by mixing equal volumes of 0.94 M sodium borohydride (NaBH<sub>4</sub>) and 0.18 M FeCl<sub>3</sub>. Iron particles were synthesized in the laboratory via the following reaction:



The borohydried solution was slowly added into the iron chloride with vigorous stirring (400rpm). Immediately after the first drop of reducing agent into iron solution, black particle appeared. Then, they were mixed for 15-20 min. yielded the maximum of black iron particles. Particles were separated from the solution by vacuum filtration using What-man cellulose nitrate membrane filter (0.2mm). Solid particles were washed three times with absolute ethanol to remove all water. This washing process is probably the key step of synthesis since it prevented the rapid oxidation of nZVI. For storage, a thin layer of ethanol added to preserve nano iron particles from oxidation.

Characterization of iron particles: The chemical composition of the synthesized nZVI was identified by X-ray fluorescence (XRF) analysis of nZVI done with JSX-3222 analyzer to analyze the main elemental compositions of the minerals that are present in iron particles. Surface morphology of particles was characterized by SEM (JEOL JSM-5600 LV). Transmission Electron Microscopy (TEM) images of the particles size distribution of n ZVI particles recorded with EM (208S Philips, Netherlands) at 80 kV, and photos were taken by digital camera (Canon, Japan). Samples prepared by depositing a few droplets of dilute iron nanoparticles solution on carbon-coated copper grids.

Effect of iron nanoparticles on *S. mansoni* adult worms: *S. mansoni* adult worms were divided into three groups, each group having 10 worms. Two groups were exposed to concentration of the iron nanoparticles (30 mg/L- 60 mg/ L) and control none exposed.

Finally, the treated worms were observed to calculate the mortality rate and then, the dead worms were prepared to SEM examination to evaluate the effect of nanoparticles.

Effect of iron nanoparticles on *Biomphalaria alexandrina* snails: Serial concentrations of iron nanoparticles were used (1, 2, 3, 4, 5, 6, 7, 8, 9, 10, 15, 20 & 40 mg/L.

Snails were exposed to the concentration for 24 hrs then, they were washed and recovered in dechlorinated tap water for another 24 hrs. Mortality rate of snails were calculated and recorded for each concentration

### Results

Characters of Iron oxide nanoparticles: The SEM images of iron oxide nanoparticles appeared as a spherical particle and formed a chain-like aggregate attributed to the magnetic interactions between the adjacent metal particles (Fig.1). The TEM images (Fig. 2), clearly showed presence of the shell layer of iron oxide and the core of nano-zero valent iron particles. Darker color represented the core while lighter one represented the shell of particles.

TEM images showed that nanoparticles were mostly spherical in shape forming chain like aggregates with particle size ranged from 30.7 to 61.4nm. Diameters average of particles was 49.4nm (±12.2nm). Elemental analysis of iron nanoparticles was performed using X-Ray fluorescence (XRF) revealed high purity of synthesized particles, 99.99% of element of composition nanoparticles was Fe (Fig. 3).

*In vitro* effects of iron nanoparticles on *S. mansoni* adult worms: The iron nanoparticles showed anti-parasitic activity against *S. mansoni* adults where at concentration 30mg/L of NPs, the mortality percentages were 15, 20 & 100% after 2, 3 & 12hrs, respectively. Besides, the exposed worms to NPs at concentration 60mg/L revealed mortality rates 55, 65, 77 and 100% at 1,2, 3,12 hours, respectively (Tab. 1).

Table1: Effects of iron nanoparticles on adult *S. mansoni* worms *in vitro*.

INP Mg/L	No. of Worms	% of dead worms /hour							
		½hr.	1hr.	2hr.	3hr.	4hr.	12hr.	24hr.	48hr.
0	7M,3F	0	0	0	0	0	0	0	0
30	5M,5F	0	0	15	20	100	100	100	100
60	6M,4F	0	55	65	77	100	100	100	100

Effects of Iron nanoparticles on *S. mansoni* adults: SEM of untreated worms showed a normal surface architecture of *S. mansoni* male worms where an intact tegument bearing large numerous tubercles with evenly distributed spines. Male tegumental structure revealed the presence of numerous large tubercles with a concentration of spines and in the areas between tubercles, the spines are evenly dispersed, and the surface is composed of circular folding with minute sensory pores (Fig. 4). Ventral sucker showed normal architecture (Fig. 5).

Exposure of adults at concentration 60mg/L of iron nanoparticles resulted in a great damage to the surface of male worm with highly deformation of the oral and ventral suckers and loss of their spines. The ventral sucker sinks incompletely inside tegumental surface. Sloughing and perforation were on body surface, (Fig. 6). Also, collapsed tegumental architecture, huge oedematous structures were sloughed from collapsed tegument (Fig. 7). The commonest surface change was exposing of blebs everywhere, cracks, erosion, and incomplete fusion of some tubercles that lost most of their spines. Perforation was notice on some areas of the tegument (Fig. 8). In other areas, the tegument showed sever lesion where sloughing of the outer tegument of layer was observed. Elsewhere, some tubercles showed incomplete fusion, distorted with short and blunt spines (Fig.9). In female worms, prominent damage was peeling of the surface in different areas, perforation and erosion. Deep cracks of the tegument were also observed (Fig. 10).

*In vitro* molluscicidal effect of iron nanoparticles: Iron nanoparticles showed a significant molluscicidal effect on *B. alexandrina*, where at very low concentration ranged from 1 to 10 mg/L, mortality percentages ranged from 4% to 43%. Snails 100% mort-

ality rate was recorded at concentration 40-mg/L after 24 hrs of exposure. Also, lethal concentration of 50% (LC<sub>50</sub>) & LC<sub>90</sub> were 12mg/L & 29mg/L, respectively (Fig. 11).

### Discussion

The presented data showed that the iron nanoparticles exhibited activity on *S. mansoni* adults, at concentration 30mg/L of iNPs, mortality rate was 15%, 20% after 2 & 3 hrs, respectively, but 100% was achieved after 12, 24 & 48 hrs. The worms exposed to iNPs at concentration 60mg/L showed mortality rates of 55%, 65%, 77% & 100%, after 1, 2, 3 & 48 hrs, respectively. These results were in accordance with results of Luz *et al* (2012). *In vitro*, they evaluated schistosomacidal activity of curcumin incorporated with poly (lactic-co-glycolic) acid (PLGA) nanoparticles, where 100% mortality was achieved at 50 & 100µM after 12 & 24hrs, respectively. Its motor activity decreased in the first 24hrs when incubated at 40µM & 30µM through 12hrs. Besides, curcumin-loaded PLGA nanoparticles caused partial alterations in adults' integument in concentrations higher than 40µM; presence of structural vesicles and alteration was showed after 48 hrs incubation. These results agreed with present data. Also, Dkhil *et al* (2016) reported that SeNPs (0.5mg/kg body weight) injection for 7 sequent days *in vivo* have antischistosomal activities in hepatic tissue of infected mice. Dorostkar *et al* (2017) found that iron nanoparticles on *Toxocara vitulorum* worms gave effects in first 6hrs with maximum pick in 12hrs. Nanoparticles activity were evidenced by increased mortality rate and decreased of worms' mobility.

In the present study, a similar result was recorded as iron nanoparticles decreased *S. mansoni* activity and increased its mortality. Pusic *et al* (2013) recommended iron oxide nanoparticles as a clinically accepted delive-

ry platform for a recombinant blood-stage human malaria vaccine.

In the present work, iron nanoparticles were effective on *B. alexandrina* with 100% mortality at 400mg/L and LC<sub>50</sub> & LC<sub>90</sub> values were at 12, & 29 mg/L, respectively. Also, Besnaci *et al* (2016) recorded the toxicity of Fe<sub>2</sub>O<sub>3</sub> nanoparticles on the *Helix aspersa* embryonic stages with different concentrations by egg membrane deformation and a low hatching rate in 12<sup>th</sup> day. But, Eduardo *et al.* (2016) reported that the magnite nanoparticles ( $\gamma$ -Fe<sub>2</sub>O<sub>3</sub>) coated with meso-2, 3-dimercaptosuccinic acid (DMSA) stabilizer affected survival and reproduction of *B. glabrata*, without significant differences between experimental and control groups (< 0.05). Shaldoum *et al.* (2016) reported that Cu<sub>2</sub>O NPs was more toxic than copper sulphate (CuSO<sub>4</sub>) against *B. alexandrina*.

### Conclusion

Perhaps, this is the first study carried out of iron nanoparticles to treat *S. mansoni* worms. No doubt, iron nanoparticles represented one of the most important veterinary tools for developing more effective low cost protocols to treat schistosomiasis.

### References

Baiocco, P, Ilari, A., Ceci, P, Orsini, S, Gramiccia, M, *et al*, 2010: Inhibitory effect of silver nanoparticles on trypanothione reductase activity and *Leishmania infantum* proliferation. ACS Med. Chem. Lett. 2, 3:230-3.

Besnaci, S, Bensoltane, S, Braia, F, Zerari, L, Khadri, S, *et al*, 2016: Embryotoxicity evaluation of iron oxide Fe<sub>2</sub>O<sub>3</sub> on land snails: *Helix aspersa*. J. Entomol. Zool. Stud. 4, 4:317-23.

Cioli, D, Pica-Mattocchia, L, Archer, S, 1993: Drug resistance in schistosomes. Parasitol. Today 9:162-6.

Delavari, M, Dalimi, A, Ghaffarifar, F, Sadraei, J, 2014: In vitro study on cytotoxic effects of ZnO nanoparticles on promastigote and amastigote forms of *Leishmania major*. Iran. J. Parasitol. 9, 1:6-13.

Dkhal, MA, Bauomy, AA, Diab, MSM, Al-Quraishy, S, 2016: Protective role of selenium nanoparticles against *Schistosoma mansoni* ind-

uced hepatic injury in mice. Biomed. Res. 27, 1: 214-9.

Dorostkar, R, Ghalavand, M, Nazarizadeh, A, Tat, M, Hashemzadeh, MS, 2017: Anthelmintic effects of zinc oxide and iron oxide nanoparticles against *Toxocara vitulorum*. Int. Nano Letters 7, 2:157-64.

Estelrich, J, Escribano, E, Queralt, J, Busquets, M, 2015: Iron oxide nanoparticles for magnetically-guided and magnetically-responsive drug delivery. Int. J. Mol. Sci. 16, 4:8070-101.

Fallon, PG, Doenhoff, MJ, 1994: Drug-resistant schistosomiasis: Resistance to praziquantel and oxamniquine induced in *Schistosoma mansoni* in mice is drug specific. Am. J. Trop. Med. 51:83-8.

Gupta, AK, Gupta, M, 2005: Synthesis and surface engineering of iron oxide nanoparticles for biomedical applications. Biomaterials 26:3995-4021

Ismail, M, Botros, S, Metwally, A, William, S, Farghally, A, 1999: Resistance to praziquantel: Direct evidence from *Schistosoma mansoni* isolated from Egyptian villagers. Am. J. Trop. Med. Hyg. 60:932-5.

Ke, Q, You-Sheng, L, Wei, W, Guo-Li, Q, Hong-Jun, L, *et al*, 2017: Studies on resistance of *Schistosoma* to praziquantel XVII Biological characteristics of praziquantel-resistant isolates of *Schistosoma japonicum* in mice. 29, 6:683-8

Khan, I, Saeed, K, Khan, I, 2017: Nanoparticles: Properties, applications and toxicities. Arabian J. Chem. 1-24.

Khan, YA, Singh, BR, Ullah, R, Shoeb, M, Naqvi, AH, *et al*, 2015: Anthelmintic effect of biocompatible zinc oxide nanoparticles (ZnO NPs) on *Gigantocotyle explanatum*, a neglected parasite of Indian Water Buffalo. PLoS ONE 10, 7: e0133086.

Kim, SW, Jung, JH, Lamsal, K, Kim, YS, Min, JS, *et al*, 2012: Antifungal effects of silver nanoparticles (AgNPs) against various plant pathogenic fungi. Mycobiol. 40, 1:53-8.

Luz, P, Magalhães, L, Pereira, A, Cunha, W, Rodrigues, V, *et al*, 2012: Curcumin-loaded in vitro PLGA nanoparticles: preparation and in vitro schistosomacidal activity. Parasitol. Res. 110: 593-8.

Mahdy, S, Raheed, Q, Kalaichelvan, P, 2012: Antimicrobial Activity of zero-valent Iron Nanoparticles. Int. J. Mod. Engin. Res.(IJMER). 2: 578-81.

**Oliveira-Filho, EC, Filho, JS, Novais, LA, Peternele, WS, Azevedo, RB, et al, 2016:** Effects of  $\gamma$ -Fe<sub>2</sub>O<sub>3</sub> nanoparticles on the survival and reproduction of *Biomphalaria glabrata* (Say, 1818) and their elimination from this benthic aquatic snail. *Environ. Sci. Pollut. Res.* 23:18362-8.

**Pusic, K, Aguilar, Z, Mc-Loughlin, J, Kobuch, S, Xu, H et al, 2013:** Iron oxide nanoparticles as a clinically acceptable delivery platform for a recombinant blood-stage human malaria vaccine. *FASEB J.* 27, 3:1153-66.

**Roduner, E, 2006:** Size matters: Why nano-materials are different? *Chem. Soc. Rev.* 35:583-92.

**Shaldoum, FM, Zayed, KM, Azzam, AM, Sharaf El Din, AT, Abou Senna, F.M, 2016:** Immunological effect of Cu<sub>2</sub>O nanoparticles on *Biomphalaria alexandrina* snail the intermediate host of *Schistosoma mansoni* in Egypt. *Curr. Sci. Int.* 5, 1:92-102.

**Sun, W, Margam, VM, Sun, L, Buczkowski, G, Bennett, GW, et al, 2006:** Genome-wide

analysis of phenobarbital-inducible genes in *Drosophila melanogaster*. *Insect Mol. Biol.* 15, 4:455-64.

**Wang, C, Liu, LL, Zhang, AT, Xie, P, Lu, JJ, et al, 2012:** Antibacterial effects of zinc oxide nanoparticles on *Escherichia coli* K 88. *Afr. J. Biotechnol.* 11, 44:10248-54.

**WHO, 2002:** First Report of the Joint WHO Expert Committees on the Prevention and Control of Schistosomiasis and Soil-transmitted Helminthes. Geneva, Switzerland

**You, J, Zhang, Y, Hu, Z, 2011:** Bacteria and bacteriophage inactivation by silver and zinc oxide nanoparticles. *Colloids Surf. B.* 85, 2: 161-7.

**Zhang SM, Coultas KA, 2011:** Identification and characterization of five transcription factors that are associated with evolutionarily conserved immune signaling pathways in the schistosome-transmitting snail *Biomphalaria glabrata*. *Mol. Immunol.* 48:1868-81.

### Explanation of figures

Fig. 1: SEM showing chain like aggregates of spherical iron nanoparticles.

Fig. 2: Transmission electron micrograph showing shell layer of iron oxide nanoparticles. Note darker core & the lighter shell of particles.

Fig. 3: X-ray fluorescence (XRF) showing main chemical elemental analysis of iron nanoparticles.

Fig. 4: SEM of tegumental surface of male *S. mansoni*, recovered from control infected mice showing enlarged papilla(P) with pore (arrowhead) and folded intertubercular tegument (arrow).

Fig. 5: SEM of ventral surface of adult male *S. mansoni* recovered from control infected mice showing normal architecture of the ventral sucker (VS) which acquire a rosette-shape (arrow).

Fig. 6: SEM of adult male *S. mansoni* worm exposed to 60 mg/L of iron nanoparticles showing damage in sucker region, deformation of the oral (OS) and ventral suckers (VS). The ventral sucker sink incompletely inside the tegumental surface, sloughing (S) was observed, perforation (P) and cracks were notice of the body surface (arrowhead).

Fig. 7: SEM of adult male *S. mansoni* worm exposed to 60 mg/L of iron nanoparticles showing collapsed tegumental architecture and huge oedematous structure (arrow).

Fig. 8: SEM of adult male *S. mansoni* worm exposed to 60 mg/L of iron nanoparticles showing numerous blebs everywhere (PL), cracks (CR), shrinkage, tubercles lost most of their spines (arrow). Note incomplete fusion of some tubercles (arrowhead). Perforation (P); notice on some tegumental areas.

Fig. 9: SEM of adult male *S. mansoni* worm exposed to 60mg/L of iron nanoparticles showing sever lesion (L) on surface. Note swelling of intertubercular spaces (arrowhead) and sloughing (S) of tegument in some area.

Fig. 10: SEM of dorsal surface of female worm exposed to 60 mg/L of iron nanoparticles showing complete damage of tegument, perforation (P) and sloughing (S). Deep cracks (arrow).

Fig. 11: Mortality rate of *B. alexandrina* snails against iron nanoparticles. LC<sub>50</sub> = 12 mg/L, LC<sub>90</sub> = 29mg.

